

Unleashing Language Models by Summarizing the Causal Factors for Counterfactual Video Question Answering

Anonymous EACL submission

Abstract

While pretrained vision and language models have shown improvement in many high-level tasks, causal and counterfactual video question answering (QA) still remains challenging. In contrast, pretrained (Large) Language Models have shown superior counterfactual reasoning abilities. In this work, therefore, we propose a natural language representation of videos that can capture objects, spatial relationships, and temporal events involving the objects; which can be more efficiently processed by pretrained Language Models for Video QA. We use this representation to capture important causal factors as additional context for Language-only models. We perform extensive experiments over two synthetic video QA datasets, namely CRIPP-VQA and CLEVERER – which covers counterfactual questions. We observe state-of-the-art results on CRIPP-VQA (upto 20% improvement in some categories) and improvement over state-of-the-art on counterfactual questions for CLEVRER. Our analysis shows the effectiveness of explicit entity-event representations for counterfactual video QA.

1 Introduction

Counterfactual Reasoning revolves around hypothetical scenarios and explores possible outcomes or consequences if certain conditions have been different. Counterfactual QA dataset is principally comprised of queries designed to delve into counterfactual or "What if" scenarios related to the intrinsic properties of objects. Properties of an object can be divided into extrinsic and intrinsic properties. Extrinsic properties of objects, encompassing shape, size, color and textures, can be easily identified with computer vision and found utility in applications such as captioning, retrieval etc. However, for Causal or Counterfactual reasoning tasks the intrinsic properties of objects such as mass, friction, elasticity, etc. must be taken into consideration. For example the Figure ...

With Video QA the modality of the data increases compared to a Language QA. Thus, the reasoning models need to preserve and understand the spatio-temporal relations between the objects. The spatio-temporal events depicted in videos such as collisions between objects hides visual cues about the intrinsic properties of these objects. Learning these video representations in multimodal setting is a struggle for the current Vision-Language models. On the contrary, extensive experiments have shown that Language models such as BERT, RoBERTa, T5 with their vast Natural Language understanding have out performed Vision-Language counterparts in every reasoning tasks. Models such as QUARTET (Rajagopal et al., 2020) and RGN (Zheng and Kordjamshidi, 2021) trained on Language only Counterfactual dataset, WIQA (Tandon et al., 2019), also provided significant evidence on this fact.

To explicitly capture such causal factors(objects, relations and events) we proposed a structured and causal model to extract video representations and convert them into a Language only structure. Extracting these video representations involves extracting each of the object's spatial relations and information as well as extracting the spatio-temporal collision events. We employed the YOLOv8 object detector to frame-wise extract each object's region proposals. These region proposals helped in building the spatial relationship graph and discover the collision events. To convert these representations into text format we proposed a visual dependency grammar. For the spatial information of an object, this grammar involves the direction of the object with respect to the origin and the nearest object. For the collision temporal event we use the collision dynamics involving the direction of approach - collision - direction of separation. We concatenate all this together to build the entity-event graph. This graph, then serves as a context for the QA based training of Language models.

083 In summary, we make the following contributions:
084

- 085 • We proposed a method that could extract
086 video representations and convert them into
087 Language only format, preserving the spatial
088 and spatio-temporal relations.
089 • Our pipeline provided a Language only solution
090 for counterfactual reasoning in Video QA
091 dataset

092 2 Related Work

093 **Image and Video Knowledge Representation.**
094 Graph-based Knowledge Representations such as
095 scene graphs (Krishna et al., 2017) and Visual
096 relationships (Lu et al., 2016) are efficient representations
097 to capture the complete set of objects and pairwise
098 relationships (including spatial and semantic)
099 between objects in an image. Researchers have also
100 extended such graph-based representations in the
101 context of videos, such as video scene graph (Yang
102 et al., 2023b), video relationship detection (Ji et al.,
103 2023, 2021). However, the method for capturing
104 such graphs are not easily generalizable to capture
105 spatio-temporal events in synthetic scenarios. For
106 example, most methods target natural images, and
107 videos; capturing commonsense events or actions,
108 such as *walking towards, lifts*; whereas in synthetic
109 videos, events are primarily collisions among
110 objects. In our work, we take inspiration from visual
111 dependency relations (Elliott and Keller, 2013) to
112 capture the spatial relationships among objects. Pri-
113 marily, this work proposes to calculate the spatial
114 relationships based on certain geometric properties,
115 overlap among objects, angle and distance between
116 regions. Temporally, we model the collision events
117 by detecting the collision dynamics consisting of
118 *approach-collide-separate* sub-events.

119 **Image Difference captioning and Video Caption-
120 ing.** Image Difference Captioning is the task of
121 identifying the difference between a pair of im-
122 ages. Models such Robust Change Captioning
123 (Park et al., 2019) and CLIP4IDC (Guo et al., 2022)
124 can be trained to identify changes between a pair
125 of images. However, the task and the datasets are
126 not targeted to capture temporal or spatial rela-
127 tionship changes. Similarly state-of-the-art image cap-
128 tioning methods fall short for two reasons: i) they
129 overtly concentrate on capturing a few salient as-
130 pects of the image, and ii) they are not trained for
131 arbitrary synthetic images. We have qualitatively

132 explored dense captioning (Johnson et al., 2016)
133 as it attempts to describe all objects present in the
134 scene. The dense captioning methods suffer from
135 similar issues such as image captioning methods
136 for lack of generalization to arbitrary videos.

137 A video dense captioning model Vid2seq (Yang
138 et al., 2023a) is an interesting baseline, that is tar-
139 geted to capture important saptio-temporal events
140 in natural videos. This has similar limitations as
141 compared to image captioning, focusing on captur-
142 ing salient events and trained for general domain
143 commonsense natural videos. Most of these tech-
144 niques do not capture necessary spatial relation-
145 ships and all important temporal events in a video.

146 **Representation and Reasoning with Pretrained
147 Vision and Language Models.** The Vision and
148 Language models (Kim et al., 2021; Li et al.,
149 2023a) and Language Models (BERT, RoBERTa,
150 T5 and LLMs such as GPT-3.5, GPT-4) have
151 seen to successfully learn task-agnostic vector-
152 ized representations that demonstrated superior per-
153 formance for both text-only, and vision and lan-
154 guage tasks. However, for counterfactual reasoning
155 (Pearl, 2009), we ideally need a structural causal
156 model describing the relationship among causal
157 factors. The task also concerns reasoning about
158 aspects not present in the observed data. Thus,
159 several work has demonstrated shortcomings in
160 counterfactual reasoning over vision and language
161 (both images and videos) (Sampat et al., 2021; Pa-
162 tel et al., 2022) Especially, for videos, Patel et al.
163 (2022) shows the best performing models achieve
164 around 70% accuracy for counterfactual questions.
165 In contrast, extensive experiments have shown that
166 smaller language models such as BART, T5 (Fro-
167 hberg and Binder, 2022; Li et al., 2023b) and Large
168 Language Models such as GPT-4 (Kiciman et al.,
169 2023) can perform causal and counterfactual rea-
170 soning with impressive performance. We, therefore,
171 look towards utilizing language models for counter-
172 factual video QA by capturing the important causal
173 factors in videos through text, primarily capturing
174 objects, spatial relationships and temporal events.

175 3 Extracting Entity-Event Representation 176 from Videos

177 The key challenge for causal and counterfactual
178 Reasoning from video datasets is preserving as
179 much of the spatial and spatio-temporal relations
180 as possible. The method should encompass extract-
181 ing informations from all the frames of the video

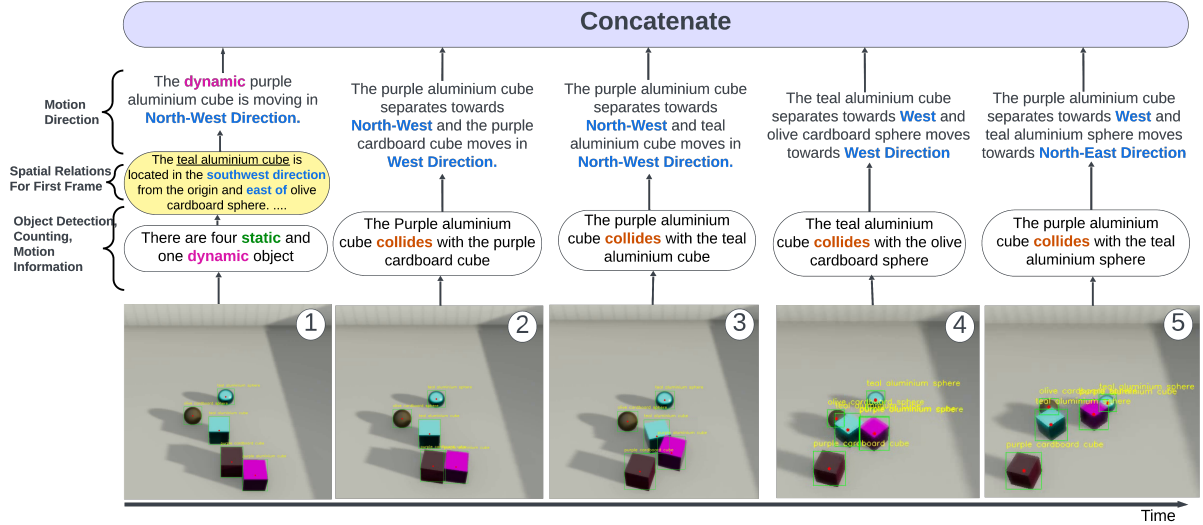


Figure 1: An example of the SUMMARY GENERATOR generating video summaries. For the initial frame, we summarize the number and type of each object, spatial relationships among pairs of objects and any motion information (with respect to next frame). For subsequent frames, we summarize the motion information and the collision information.

and not just the salient feature of the video. In this Section, we propose an efficient video representation that can be processed by powerful Language Models, and discuss how to efficiently extract from the videos. Consider Figure 1 as a running example. We are breaking down the example into key frames and their representations.

- **Frame 1:** Description of the static and dynamic objects and spatial relationships among the objects.
- **Frame 2:** Collision between purple aluminium cube and purple cardboard cube along with their directions of approach and separations.
- **Frame 3:** Collision between purple aluminium cube and teal aluminium cube along with their directions of approach and separations.
- **Frame 4:** Collision between teal aluminium cube and olive cardboard sphere along with their directions of approach and separations.
- **Frame 5:** Collision between purple aluminium cube and teal aluminium sphere along with their directions of approach and separations.

3.1 Extracting Video Representations

We aim to create an efficient and comprehensive representation of visual information in video to reason about spatio-temporal events in a causal and counterfactual manner. To this end, our representation involves per-frame representation of objects, spatial relations and temporal events across frames.

Representing & Extracting Object, Spatial Relationships. To create a graph for video representation, the first thing we need is to get both the information and the location of the objects present in the video. Extracting this information is done by object detection models such as YOLO (Redmon et al., 2016). After the extraction process, the next job is to efficiently represent the objects as well as their spatial relationships. Our proposed approach hinges on structured dependency representations of images.

The localization of an object is done by establishing its direction from the nearest two objects or it's direction from the nearest object and the direction with respect to the origin. An illustration of this concept can be encapsulated in this statement, *The pen is positioned upon the table and adjacent to the box*. This method will convert the spatial information about each of the objects into structured textual format. For example, consider the Figure

This figure shows the spatial information of one such object. To build the graph we need the spatial information of every static and dynamic object.

Representing & Extracting Collision Events. The next part of building the video representation graph is preserving the spatio-temporal relations of all the objects. The temporal event for the synthetic datasets such as CRIPP-VQA (Patel et al., 2022) and CLEVRER (Yi et al., 2020) is "Collision" between the various objects. To extract out

182
183
184
185
186
187
188
189
190
191
192
193
194
195
196
197
198
199
200
201
202

210
211
212
213
214
215
216
217
218
219
220
221
222
223
224
225
226
227
228
229
230
231
232

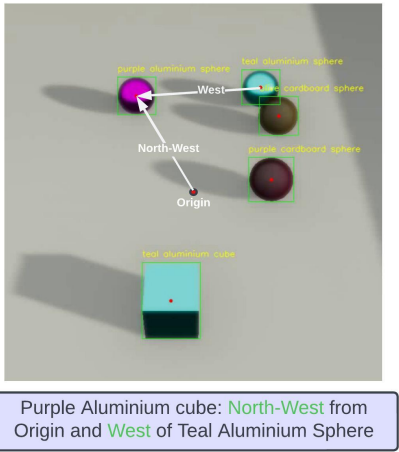


Figure 2: For each pair of objects, based on the bounding boxes, we capture spatial relationships. We use ordinal directions to describe the relationships, as LMs may acquire the commonsense understanding of such directions during pretraining (Tarunesh et al., 2021).

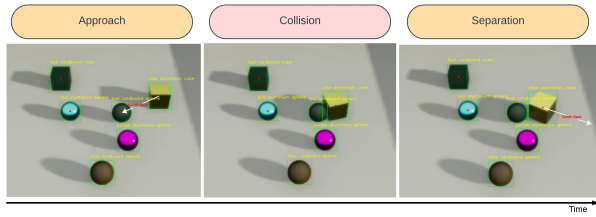


Figure 3: Any collision event can be decomposed into *approach*, *collide* and then *separation* subevents.

the collision events we need to observe the locations of each objects. A collision event will result in an overlapping of the location coordinates. The Figure below demonstrates the difference between the collisions and no-collisions. It also marks the direction of the dynamic object which is required for the next stage of the process.

3.2 Efficient Video Representation

From the previous sections we got the building blocks for the video representation graph. We have done this representation by concatenation of two parts: spatial information of the objects and spatio-temporal relations of the objects.

Building the graph. After the extraction of the collision events, the spatio-temporal relations are obtained by delineating those events for both the "collider" and "collidee". We need to preserve the dynamics of approach and separation. This entails the consideration of the respective motion and directionality for both "collider" and "collidee" ob-

jects. Figure 3 shows the dynamics of Collisions. We have implemented the same approach of directional cues into textual format encoding. Finally, to build the graph we need to concatenate the spatial informations with these spatio-temporal relations.

4 Experiments

4.1 Entity-Event Extraction

The extraction of salient entities and events helps to generate an efficient object-centric representation of the visual context in videos to help the model focus on the information relevant to question answering. To this end, we employ a YOLOv8 (Redmon et al., 2016) (Jocher et al., 2023) detector to extract frame-wise object proposals. In order to add temporal context, we analyze the change in position of objects across successive frames and note the variation of motion directions over time. An illustration of our context generation approach is shown in Figure 1. We describe the initial state of objects by their relative position in terms of direction with respect to the center of the frame. Moreover, for dynamic objects, we incorporate the initial movement directions while entering the scene or at the beginning of motion. In addition to an initial description of the static and dynamic objects, we also detect key collision events under the assumption that **objects collide when their bounding boxes overlap significantly**. Our description of a collision event involves the colliding objects involved (*collider* and *collidee*) and the motion directions after collision.

Specifying the relative initial state of objects and motion directions along with the extraction of collisions allows for a succinct representation of the key events and the causal factors which govern them, allowing text-only language models to reason effectively even in case of more challenging counterfactual scenarios. Further analysis on the context generation quality is provided in Section 5.2.2.

4.2 Datasets

We evaluate the performance of our approach on the CRIPP-VQA (Patel et al., 2022) and CLEVRER (Yi et al., 2020) datasets.

CRIPP-VQA aims to test the model's understanding of implicit physical properties based on learning from videos. It consists of 5000 videos and 93,962 questions depicting standard-shaped

308 moving objects with implicit physical properties
309 like mass and friction interacting with each other
310 through collisions. Questions are divided into three
311 types - DESCRIPTIVE (41,761 questions), COUN-
312 TERFACTUAL (41,761 questions) and PLANNING
313 (10,440 questions), in which counterfactual ques-
314 tions involve three possible object manipulation
315 scenarios - *Add* (27,016 questions), *Remove* (9603
316 questions) and *Replace* (5142 questions) objects in
317 videos.

318 **CLEVRER** evaluates causal and temporal rea-
319 soning for videos based on physics simulations. It
320 consists of 20,000 videos and 305,910 questions
321 depicting object shapes interacting through colli-
322 sions in a simulation environment. The dataset
323 aims to test model reasoning through four types
324 of questions - DESCRIPTIVE (219,918 questions),
325 EXPLANATORY (33,811 questions), COUNTERFAC-
326 TUAL (37,253 questions) and PREDICTIVE (14,298
327 questions).

328 4.3 Baseline methods

329 Pre-trained transformer-based models (Devlin et al.,
330 2019), in conjunction with visual encoders (He
331 et al., 2018), have been extensively used in cre-
332 ating state-of-the-art models for joint visual and
333 textual reasoning owing to their ability to handle
334 inputs pertaining to diverse modalities with large
335 context lengths (Liu et al., 2021b) (Carion et al.,
336 2020). However, since our approach involves the
337 representation of video features using textual sum-
338 maries, we employ the text-only T5 (Raffel et al.,
339 2023) architecture, a state-of-the-art large language
340 model which shows strong performance in various
341 natural language tasks. We conduct our evalua-
342 tion on two T5 variants: T5-*base* (223M parameters)
343 and T5-*large* (783M parameters) and explore both
344 *rule-based* and *triplet-based* contextual configura-
345 tions.

346 We compare our approach to a combination
347 of text-only and visual-language models on the
348 CRIPP-VQA dataset :

349 **Blind-T5** refers to the T5-base model, which
350 processes only questions as input. We employ this
351 baseline to analyze textual biases in the dataset.

352 **YOLOv8-T5_{summary}** consists of the YOLOv8 and
353 T5 models with rule-based summaries as video
354 context.

355 **YOLOv8-T5_{triplets}** consists of the YOLOv8 and
356 T5 models with triplet-based summaries as video

357 context.

358 **Aloe*-BERT** is a state-of-the-art video-language
359 model which consists of a modified MaskRCNN-
360 based Aloe visual encoder (Ding et al., 2021)
361 (He et al., 2018) to detect object proposals, a
362 pretrained BERT (Devlin et al., 2019) encoder
363 to generate question embeddings and a learnable
364 BERT component for question answering. We
365 use the Aloe*-BERT model as specified by (Patel
366 et al., 2022) and benchmark our approach’s results
367 against it for the CRIPP-VQA dataset tasks.

368 Similarly, for the CLEVRER dataset, we
369 contrast the performance of our approach against
370 the following baseline models specified in (Yi et al.,
371 2020) which rely on both visual and language
372 inputs.

373 **CNN+LSTM** extracts visual video features via
374 a convolutional neural network (CNN) and uses
375 pretrained Word2vec (Mikolov et al., 2013) embed-
376 dings for encoding questions, which are then sent
377 to an LSTM (Hochreiter and Schmidhuber, 1997)
378 for answer prediction.

379 **MAC** (Hudson and Manning, 2018) incorporates a
380 joint attention mechanism on both the image fea-
381 ture map and the question. (Yi et al., 2020) employ
382 a modified version of the model by integrating a
383 temporal attention unit across frames to generate a
384 latent video embedding (**MAC (V)**).

385 **NS-DR** (Yi et al., 2020) is a state-of-the-art
386 video-language model which uses a dynamics
387 predictor, a learnable physics engine which inputs
388 object proposals from a visual encoder and learns
389 the variation of object dynamics across frames for
390 predicting motion directions and collision events.

395 4.4 Implementation details

396 We employ the following procedures for testing
397 our approach’s performance on the CRIPP-VQA
398 and CLEVRER datasets :

399 **T5:** For the CRIPP-VQA dataset, we leverage
400 a randomly-sampled 67.5:22.5:10 train:val:test
401 split of the set of question-answer pairs for each
402 task in the IID set. Moreover, for CLEVRER
403 we employ a 3:1 ratio of the train set for train
404 and validation splits and the original validation
405 set as the held-out test set. The video frames are
406 sampled at 25FPS and passed through a YOLOv8

model **finetuned on a small set of 150 manually annotated training examples?** to extract the visual features. The extracted visual features were then passed through the SUMMARY GENERATOR to generate tuples $\{c_i, q_i, a_i\}$, where c_i is the generated video context, q_i is the question and a_i is the answer. In case of multi-choice questions, we apply the same procedure to create tuples for each option, effectively reformulating the multi-choice question into a set of option-wise binary single choice questions. For both the *base* and *large* versions, we use the corresponding pretrained T5 tokenizer, setting the maximum question length $q_{len} = 1024$ and answer length $t_{len} = 32$. with lr = $1e^{-5}$ is used. For each task, the model was trained using Adam optimizer (Kingma and Ba, 2017) for 10 epochs with a batch size of 2 on a single 32GB Nvidia V100 GPU for 16 hours.

Aloe*-BERT: The Aloe*-BERT module consists of three components - (1) a visual encoder, (2) a pretrained textual encoder and (3) a large language model (LLM). The model utilizes extracted visual features from videos and textual embeddings from questions in the CRIPP-VQA dataset to predict answers. We use a modified version of the Aloe (Ding et al., 2021) module called Aloe* for visual feature extraction as specified by (Patel et al., 2022) in which the MONet (Burgess et al., 2019) module is replaced by Mask-RCNN (He et al., 2018). The video frames are sampled at 25FPS and forwarded through the Aloe* module with a linear layer f_v to generate frame embeddings u_v of dimension $d = 768$. The questions and answers are passed through a pretrained BERT encoder and a linear layer f_t to generate textual embeddings u_t of dimension $d = 768$. The visual and textual features are then concatenated and passed as input to a BERT model for question answering.

We finetune the BERT model with RAdam (Liu et al., 2021a) optimizer using a linear schedule with lr = $5e^{-6}$ and warmup steps = 4000. The model is initially trained for 6 hours on the descriptive task and then finetuned for 14 hours on a combined task of descriptive and counterfactual questions, each for 25 epochs. Subsequently, the trained descriptive checkpoint is further finetuned on the counterfactual and planning tasks each for 50 epochs and 6 hours. The training is done with a batch size = 64 on two 32 GB Nvidia V100 GPUs.

4.5 Evaluation metrics

For the CLEVRER and CRIPP-VQA datasets, we adopt the per-question (PQ) accuracy for all types of tasks. Moreover, for explanatory, counterfactual and predictive tasks which involve multiple-choice answers, we reformat the questions in terms of binary True-False sub-questions for each option, employing the per-option (PO) accuracy for evaluating option-wise correctness. For CRIPP-VQA, we report the results on the aforementioned test split, while for CLEVRER, we report the results on the original validation split.

5 Results

In this section, we demonstrate the relative performance of our approach over various state-of-the-art baselines on the CRIPP-VQA and CLEVRER datasets. Subsequently, we conduct an ablation study detailing the rationale behind the design choices employed for the SUMMARY GENERATOR.

5.1 Finetuning performance on Video-QA

We employ two types of video summaries - (1) rule-based, and (2) triplets and evaluate their effectiveness with the T5-*base* and *large* versions for video-based question answering. We contrast our approach to Aloe*-BERT on CRIPP-VQA tasks and the baselines mentioned in Section 4.3 on CLEVRER tasks.

Table 1 shows the experimental results on the CRIPP-VQA dataset for the aforementioned scenarios. Our approach outperforms Aloe*-BERT by 20.7% in terms of PO accuracy for the descriptive task, and by 10.2% and 17.2% on the counterfactual and planning tasks respectively. This indicates that the extraction of key entities and events for context generation significantly improves the large language model’s ability to develop an efficient object-centric comprehension of the video events without explicitly using visual features. Consequently, it not only helps the model attend to relevant visual information for answering descriptive queries but also allows it to engage in counterfactual reasoning and deduce potential actions aimed at specific objectives in the context of planning tasks.

A similar trend is observed for the *Add*, *Remove* and *Replace* sub-tasks where our method outperforms Aloe*-BERT by 7 – 10% and 10 – 13% on PO and PQ accuracy respectively. The results also

Model	Descriptive		Remove		Replace		Add		Counterfactual	Planning
	PO	PQ	PO	PQ	PO	PQ	Avg. PO			
Blind-T5	56.03	52.44	21.13	47.95	14.86	51.26	15.24	49.8	7.44	
Alce ³ +BERT	71.04	65.46	33.64	56.76	22.07	67.43	39.71	63.21	32.61	
T5+Metadata (base)	81.42	70.94	40.36	60.19	31.23	68.92	41.56	68.35	41.64	
YOLOv8-T5 _{triplets} (base)	90.73	70.81	42.63	67.03	35.95	73.68	46.01	72.18	46.39	
YOLOv8-T5 _{summary} (base)	88.98	72.56	44.88	65.72	34.6	74.24	47.12	72.78	47.94	
YOLOv8-T5 _{summary} (large)	91.73	72.61	45.95	65.91	35.73	75.20	48.59	73.43	49.85	

Table 1: Video-QA accuracy of visual reasoning models on CRIPP-VQA

Model	Descriptive	Explanatory PO	Explanatory PQ	Predictive PO	Predictive PQ	Counterfactual PO	Counterfactual PQ
Blind-T5	34.41	59.56	16.57	50.35	23.28	51.31	8.26
CNN+LSTM	51.8	62.0	17.5	57.9	31.6	61.2	14.7
MAC (V)	85.6	59.5	12.5	51.0	16.5	54.6	13.7
NS-DR	88.1	87.6	79.6	82.9	68.7	74.1	42.2
YOLOv8-T5 _{base}	81.96	93.22	83.13	76.51	40.94	74.45	35.74
YOLOv8-T5 _{large}	83.31	93.24	83.18	76.54	42.31	78.67	45.40

Table 2: Video-QA accuracy of visual reasoning models on CLEVRER

Model	Descriptive	Remove PO	Replace PO	Add PO	Counterfactual PO	Planning
Blind-T5	56.03	52.44	47.95	51.26	49.8	7.44
collisions-only	89.64	69.13	58.96	69.39	66.88	42.2
add-positions	88.96	70.27	63.74	71.4	68.89	44.35
collisions-directions	89.66	69.39	62.8	70.72	68.01	45.76
YOLOv8-T5 _{base}	88.98	72.56	65.72	74.24	72.78	47.94

Table 3: Ablation results for the T5-base model tested on rule-based summaries

508 indicate that models generally perform better on
509 the *Add* and *Remove* tasks compared to the *Replace*
510 task, since it involves the *in-situ* change in physical
511 properties of an object in the video frames. This im-
512 plies that the baseline models, in general, are some-
513 what able to reason spatially, but are found lacking
514 at reasoning about changes in physical properties.

515 A comparison between both summary genera-
516 tion approaches as highlighted in Table 1 shows
517 that the rule-based summary approach performs
518 on par with the triplet-based approach on the de-
519 scriptive and counterfactual tasks but achieves a
520 significant 3.5% gain for the planning task, suggest-
521 ing that LLMs like T5 are better at comprehending
522 fully textual contexts compared to triplet-based
523 scene descriptions.

524 The experimental results of visual reasoning
525 models on the CLEVRER dataset is shown in Table
526 2. Our approach outperforms the state-of-the-art
527 NS-DR model on the explanatory and counterfac-
528 tual tasks but surprisingly underperforms by a sig-
529 nificant margin on the descriptive and predictive
530 tasks. This can be attributed to the fact that the
531 NS-DR approach incorporates a dynamics planner
532 which is a learnable physics engine for explicitly
533 modelling the motion of objects over short time

frames and predicting future motion traces. This
534 not only allows for a more intricate scene represen-
535 tation which positively impacts the model’s perfor-
536 mance on the descriptive tasks but also enables it to
537 predict future events with better accuracy. Never-
538 theless, our approach still outperforms NS-DR by
539 6% and 4% in PO accuracy on the explanatory and
540 counterfactual tasks respectively while employing
541 a relatively simpler and efficient approach for vi-
542 sual context representation, suggesting that large
543 language models trained for video-QA tasks us-
544 ing fully textual descriptions of key entities and
545 events can exhibit competitive (and sometimes su-
546 perior) causal and counterfactual reasoning capa-
547 bilities over more sophisticated event modelling
548 approaches.

5.2 Ablation Studies

551 To investigate the overall effectiveness of our pro-
552 posed approach, we analyze the OBJECT DE-
553 TECTOR and the SUMMARY GENERATOR
554 and their effect on the overall context quality.

5.2.1 OBJECT DETECTOR

555 To extract moving objects from video frames,
556 we employ YOLOv8 as an object detector by

558 finetuning the model on a small set of manually
 559 annotated video frames from the CRIPP-VQA and
 560 CLEVRER datasets. Since the context quality
 561 depends on the accuracy of localization of objects
 562 per frame, we analyze the performance of our
 563 object detector by evaluating the mAP scores for
 564 both datasets as shown in Table 4. Our visual
 565 extractor achieves a high mAP score of **88.6%??**
 566 on 12 classes of the CRIPP-VQA dataset and
 567 93.4% on 48 classes of the CLEVRER dataset
 568 indicating the accurate detection of salient objects
 569 in video frames.
 570

Dataset	# classes	mAP
CRIPP-VQA	12	0.886 FIX!
CLEVRER	48	0.934

Table 4: mAP scores for YOLOv8

5.2.2 SUMMARY GENERATOR

We analyse the impact of including different types of spatio-temporal information in video contexts on the overall context quality. We consider the following scenarios.

- i) **Blind-T5** : T5-base model with no context provided, only questions as input.
- ii) **collisions-only** : context with no relative initial positions or motion directions provided, only the initial objects and collider-collidee pairs mentioned.
- iii) **add-positions**: The context consists of the initial objects, their relative initial positions with respect to the frame center and the collider-collidee pairs mentioned. We remove motion directions.
- iv) **collisions-directions**: The context consists of only the initial objects, motion directions and collider-collidee pairs mentioned. We remove relative initial positions.

The PO accuracy results for each of these scenarios are compared with the T5-base model for rule-based summaries, as shown in Table 3. Blind-T5 exhibits close to random PO accuracy performance (49.8%) on counterfactual tasks and subpar performance (7.44%) on the planning task due to the absence of contextual information. A slightly better performance is observed for the descriptive task

(56.03%), indicating that the descriptive task suffers from slight textual biases allowing the model to predict correct answers based on the question itself.

The addition of video summary as context leads to a steep increase in accuracy across all tasks (17% for counterfactual, 33% for descriptive and 34.8% for planning), highlighting the importance of contextual information in question answering. Furthermore, for dynamic scenarios involving moving constituents and collisions, the presence of spatio-temporal information like relative initial positions and motion directions greatly improves the model’s ability to understand the complex physical interactions and reason about possible steps towards a planning objective. This is substantiated by both *add-positions* and *collisions-directions* outperforming *collisions-only* by 1 – 2% on counterfactual tasks and by 2 – 3% on the planning tasks. However, the performance on descriptive questions remains relatively similar across all context variations, suggesting that the descriptive task relies less on spatio-temporal information and more on textual information for question answering.

Furthermore, a more significant performance gain is observed for the *Add* and *Replace* tasks when the complete context is provided (6% and 5% on the *Replace* and *Add* tasks respectively) compared to the *Remove* task (3%). This corroborates our experimental results on the CRIPP-VQA dataset in Section 5.1 that models typically find it challenging to analyze scenarios involving in-place changes in physical properties and suggests that the *Add* and *Replace* tasks benefit from a combination of

6 Conclusion

References

- Christopher P. Burgess, Loic Matthey, Nicholas Watters, Rishabh Kabra, Irina Higgins, Matt Botvinick, and Alexander Lerchner. 2019. *Monet: Unsupervised scene decomposition and representation*.
- Nicolas Carion, Francisco Massa, Gabriel Synnaeve, Nicolas Usunier, Alexander Kirillov, and Sergey Zagoruyko. 2020. *End-to-end object detection with transformers*.
- Jacob Devlin, Ming-Wei Chang, Kenton Lee, and Kristina Toutanova. 2019. *Bert: Pre-training of deep bidirectional transformers for language understanding*.
- David Ding, Felix Hill, Adam Santoro, Malcolm Reynolds, and Matt Botvinick. 2021. *Attention over*

650	learned object embeddings enables complex visual reasoning.	702
651		703
652	Desmond Elliott and Frank Keller. 2013. Image description using visual dependency representations.	704
653	In <i>Proceedings of the 2013 Conference on Empirical Methods in Natural Language Processing</i> , pages	705
654	1292–1302, Seattle, Washington, USA. Association	706
655	for Computational Linguistics.	707
656		708
657		
658	Jörg Frohberg and Frank Binder. 2022. CRASS: A	709
659	novel data set and benchmark to test counterfactual	710
660	reasoning of large language models.	
661	In <i>Proceedings of the Thirteenth Language Resources and Evaluation Conference</i> , pages 2126–2140, Marseille, France.	
662	European Language Resources Association.	
663		
664	Zixin Guo, Tzu-Jui Wang, and Jorma Laaksonen. 2022.	711
665	CLIP4IDC: CLIP for image difference captioning.	712
666	In <i>Proceedings of the 2nd Conference of the Asia-Pacific Chapter of the Association for Computational Linguistics and the 12th International Joint Conference on Natural Language Processing (Volume 2: Short Papers)</i> , pages 33–42, Online only. Association for	713
667	Computational Linguistics.	714
668		715
669		716
670		717
671		
672	Kaiming He, Georgia Gkioxari, Piotr Dollár, and Ross	718
673	Girshick. 2018. Mask r-cnn.	719
674		720
675	Sepp Hochreiter and Jürgen Schmidhuber. 1997.	721
676	Long short-term memory. <i>Neural Comput.</i> , 9(8):1735–1780.	722
677		723
678		724
679	Drew A. Hudson and Christopher D. Manning. 2018.	725
	Compositional attention networks for machine reasoning.	
680	Jingwei Ji, Rishi Desai, and Juan Carlos Niebles. 2021.	726
681	Detecting human-object relationships in videos.	727
682	In <i>2021 IEEE/CVF International Conference on Computer Vision, ICCV 2021, Montreal, QC, Canada, October 10-17, 2021</i> , pages 8086–8096. IEEE.	728
683		729
684		730
685	Xiaofeng Ji, Jin Chen, and Xinxiao Wu. 2023. Counterfactual inference for visual relationship detection	731
686	in videos.	732
687	In <i>IEEE International Conference on Multimedia and Expo, ICME 2023, Brisbane, Australia, July 10-14, 2023</i> , pages 162–167. IEEE.	733
688		
689		
690	Glenn Jocher, Ayush Chaurasia, and Jing Qiu. 2023.	734
691	YOLO by Ultralytics.	735
692		736
693	Justin Johnson, Andrej Karpathy, and Li Fei-Fei. 2016.	737
694	Densecap: Fully convolutional localization networks	
695	for dense captioning.	
696	In <i>2016 IEEE Conference on Computer Vision and Pattern Recognition, CVPR 2016, Las Vegas, NV, USA, June 27-30, 2016</i> , pages	
697	4565–4574. IEEE Computer Society.	
698	Emre Kiciman, Robert Ness, Amit Sharma, and Chen-	742
699	hao Tan. 2023. Causal reasoning and large language	743
700	models: Opening a new frontier for causality. <i>CoRR</i> ,	744
701	abs/2305.00050.	745
		746
		747
		748
	Wonjae Kim, Bokyung Son, and Ildoo Kim. 2021. Vilt:	
	Vision-and-language transformer without convolution or region supervision.	
	In <i>Proceedings of the 38th International Conference on Machine Learning, ICML 2021, 18-24 July 2021, Virtual Event</i> , volume	
	139 of <i>Proceedings of Machine Learning Research</i> , pages 5583–5594. PMLR.	
	Diederik P. Kingma and Jimmy Ba. 2017. Adam: A	
	method for stochastic optimization.	
	Ranjay Krishna, Yuke Zhu, Oliver Groth, Justin Johnson,	711
	Kenji Hata, Joshua Kravitz, Stephanie Chen,	712
	Yannis Kalantidis, Li-Jia Li, David A. Shamma,	713
	Michael S. Bernstein, and Li Fei-Fei. 2017. Vi-	714
	sual genome: Connecting language and vision using	715
	crowdsourced dense image annotations. <i>Int. J. Comput. Vis.</i> , 123(1):32–73.	716
		717
	Junnan Li, Dongxu Li, Silvio Savarese, and Steven C. H.	
	Hoi. 2023a. BLIP-2: bootstrapping language-image	
	pre-training with frozen image encoders and large	
	language models.	
	In <i>International Conference on Machine Learning, ICML 2023, 23-29 July 2023, Honolulu, Hawaii, USA</i> , volume 202 of <i>Proceedings of Machine Learning Research</i> , pages 19730–19742. PMLR.	
	Liunian Harold Li, Jack Hessel, Youngjae Yu, Xiang	718
	Ren, Kai-Wei Chang, and Yejin Choi. 2023b. Sym-	719
	bolic chain-of-thought distillation: Small models can	720
	also "think" step-by-step.	721
	In <i>Proceedings of the 61st Annual Meeting of the Association for Computational Linguistics (Volume 1: Long Papers), ACL 2023, Toronto, Canada, July 9-14, 2023</i> , pages 2665–2679. Association for Computational Linguistics.	722
		723
		724
		725
	Liyuan Liu, Haoming Jiang, Pengcheng He, Weizhu	726
	Chen, Xiaodong Liu, Jianfeng Gao, and Jiawei Han.	727
	2021a. On the variance of the adaptive learning rate	728
	and beyond.	729
		730
		731
		732
		733
	Ze Liu, Yutong Lin, Yue Cao, Han Hu, Yixuan Wei,	734
	Zheng Zhang, Stephen Lin, and Baining Guo. 2021b.	735
	Swin transformer: Hierarchical vision transformer	736
	using shifted windows.	737
	Cewu Lu, Ranjay Krishna, Michael S. Bernstein, and	742
	Li Fei-Fei. 2016. Visual relationship detection with	743
	language priors.	744
	In <i>Computer Vision - ECCV 2016 - 14th European Conference, Amsterdam, The Netherlands, October 11-14, 2016, Proceedings, Part I</i> , volume 9905 of <i>Lecture Notes in Computer Science</i> , pages 852–869. Springer.	745
		746
		747
		748
	Tomas Mikolov, Kai Chen, Greg Corrado, and Jeffrey	749
	Dean. 2013. Efficient estimation of word representa-	750
	tions in vector space.	751
	Dong Huk Park, Trevor Darrell, and Anna Rohrbach.	752
	2019. Robust change captioning.	753
	In <i>Proceedings of the IEEE/CVF International Conference on Computer Vision</i> , pages 4624–4633.	754
		755

756	Maitreya Patel, Tejas Gokhale, Chitta Baral, and Yezhou Yang. 2022. Cripp-vqa: Counterfactual reasoning about implicit physical properties via video question answering.	and Pattern Recognition, CVPR 2023, Vancouver, BC, Canada, June 17-24, 2023, pages 18675–18685. IEEE.	813
757			814
758			815
759			
760	Judea Pearl. 2009. <i>Causality: Models, Reasoning and Inference</i> , 2nd edition. Cambridge University Press, USA.		
761			
762			
763	Colin Raffel, Noam Shazeer, Adam Roberts, Katherine Lee, Sharan Narang, Michael Matena, Yanqi Zhou, Wei Li, and Peter J. Liu. 2023. Exploring the limits of transfer learning with a unified text-to-text transformer.		
764			
765			
766			
767			
768	Dheeraj Rajagopal, Niket Tandon, Peter Clark, Bhavana Dalvi, and Eduard Hovy. 2020. What-if I ask you to explain: Explaining the effects of perturbations in procedural text. In <i>Findings of the Association for Computational Linguistics: EMNLP 2020</i> , pages 3345–3355, Online. Association for Computational Linguistics.		
769			
770			
771			
772			
773			
774			
775	Joseph Redmon, Santosh Divvala, Ross Girshick, and Ali Farhadi. 2016. You only look once: Unified, real-time object detection.		
776			
777			
778	Shailaja Keyur Sampat, Akshay Kumar, Yezhou Yang, and Chitta Baral. 2021. CLEVR_HYP: A challenge dataset and baselines for visual question answering with hypothetical actions over images. In <i>Proceedings of the 2021 Conference of the North American Chapter of the Association for Computational Linguistics: Human Language Technologies</i> , pages 3692–3709, Online. Association for Computational Linguistics.		
779			
780			
781			
782			
783			
784			
785			
786			
787	Niket Tandon, Bhavana Dalvi, Keisuke Sakaguchi, Peter Clark, and Antoine Bosselut. 2019. WIQA: A dataset for “what if...” reasoning over procedural text. In <i>Proceedings of the 2019 Conference on Empirical Methods in Natural Language Processing and the 9th International Joint Conference on Natural Language Processing (EMNLP-IJCNLP)</i> , pages 6076–6085, Hong Kong, China. Association for Computational Linguistics.		
788			
789			
790			
791			
792			
793			
794			
795			
796	Ishan Tarunesh, Somak Aditya, and Monojit Choudhury. 2021. Lonli: An extensible framework for testing diverse logical reasoning capabilities for NLI. <i>CoRR</i> , abs/2112.02333.		
797			
798			
799			
800	Antoine Yang, Arsha Nagrani, Paul Hongsuck Seo, Antoine Miech, Jordi Pont-Tuset, Ivan Laptev, Josef Sivic, and Cordelia Schmid. 2023a. Vid2seq: Large-scale pretraining of a visual language model for dense video captioning. In <i>IEEE/CVF Conference on Computer Vision and Pattern Recognition, CVPR 2023, Vancouver, BC, Canada, June 17-24, 2023</i> , pages 10714–10726. IEEE.		
801			
802			
803			
804			
805			
806			
807			
808	Jingkang Yang, Wenxuan Peng, Xiangtai Li, Zujin Guo, Liangyu Chen, Bo Li, Zheng Ma, Kaiyang Zhou, Wayne Zhang, Chen Change Loy, and Ziwei Liu. 2023b. Panoptic video scene graph generation. In <i>IEEE/CVF Conference on Computer Vision</i>		
809			
810			
811			
812			